REGULAR PAPER

Effect of dehydration time and air tightness on pore distribution of potassium and metakaolin-based geopolymer

Japanese Journal of Applied Physics **61**, SB1003 (2022) **REGULAR PAPER**
https://doi.org/**10.35848/1347-4065/ac340d**

Effect of dehydration time and air tightness on pore distribution of potassium and metakaolin-based geopolymer

Yaru Yang[1*], Thi-Chau-Duyen Le[1], Isamu Kudo[2,3], Thi-Mai-Dung Do[1], Koichi Niihara[1], and Hisayuki Suematsu[1]

[1]*Extreme Energy-Density Research Institute, Nagaoka University of Technology, 1603-1 Kamotomioka-cho, Nagaoka, Niigata 940-2188, Japan*
[2]*Department of Nuclear System Safety Engineering, Nagaoka University of Technology, 1603-1 Kamotomioka-cho, Nagaoka, Niigata 940-2188, Japan*
[3]*ADVAN ENG. Co., ltd.3399-34, Shimami-cho, Kata-ku, Niigata 950-3102, Japan*

[*]E-mail: yyr922405@gmail.com

Received July 30, 2021; revised October 3, 2021; accepted October 27, 2021; published online January 20, 2022

As a catalyst support in the nuclear waste containers in the Fukushima Daiichi Nuclear Power Station, geopolymer is required to show high strength, high porosity and durability. The aim of this study is to evaluate the mechanical properties and pore size distribution of hardened samples based on two test variables, which include early-age dehydration time and air tightness. The early-age dehydration time ranges from 1–4 d, and air tightness is implemented using the two methods of total sealing and air contact. However, the average pore size was around 2.0×10^2 μm, the Vickers hardness was around 90 MPa, and the relative weight change on the 14th day was within 10% for all the samples that were not affected by the curing time and air tightness. It can be inferred that the pores of the sample may have been formed within a day and may not be affected by the curing time.

1. Introduction

The Fukushima Daiichi Nuclear Power Plant failed to cool down the nuclear fuels in the reactor core due to a huge earthquake and tsunami. A large amount of spent fuel melted into the cooling water, and radiolysis of the water due to the radioactive contamination produced hydrogen and oxygen. The accumulation of hydrogen may cause hydrogen explosion, and preventing hydrogen explosions has been an issue in the study of waste storage.[1)] The fine radioactive waste particles combine with water to form a slurry, so it is difficult to remove the water.[2)]

During the decommissioning of Three Mile Island Unit 2 (TMI-2), radioactive waste and water were processed and stored in tanks with Pd-Pt-Al_2O_3 catalyst to promote hydrogen and oxygen recombination.[3)] On the other hand, the Fukushima Daiichi Nuclear Power Plant must operate multiple radionuclide removal and other water treatment systems, which will generate a lot more water-carrying radioactive waste than the one of TMI-2.[2)] Therefore, it is very important to develop a cost-friendly catalyst and a support composed of metal or inorganic materials and have long-term chemical stability.

Geopolymers are inorganic alumina-silicate materials, prepared by mixing metakaolin powder or another aluminosilicate rich in silica and alumina and alkali activators, such as sodium hydroxide (NaOH) or potassium hydroxide (KOH) and sodium silicate (Na_2SiO_3) or potassium silicate (K_2SiO_3).[4)] Geopolymers have excellent physical and chemical properties, such as high compressive strength,[5–10)] low shrinkage,[11)] low thermal conductivity[12,13)], and alkali or acidic condition resistance.[14–16)] Geopolymer can be hardened at temperatures below 100 °C and a large variety of inexpensive raw materials (clay, metakaolin and certain industrial waste) can be used for geopolymer production.[5,17–20)] Consequently, geopolymers have been developed as candidate materials for hydrogen recombination catalyst support in previous research.[2,21)]

The mechanical strength of geopolymers is strongly affected by the content of K_2O and the water coefficient of H_2O/metakaolin, while the compressive strength value of the sample is not significantly different from the SiO_2 to K_2O molar ratio variable.[22)] When a sample is cured at a high temperature, compared to one cured at room temperature, the higher curing temperature will increase the early compressive and flexural strength, and even reach the target value within 1 d. In addition, the effect of temperature depends on the curing time. Curing for only 1 h at elevated temperatures will not cause a significant change in strength development, but a longer treatment time will significantly accelerate the reaction rate and increase the early strength. However, higher curing temperatures above 80 °C have a negative impact on the development of hardened geopolymers.[23)] Geopolymers contain pores and penetration of external species occurs through the pore network.[24)] The strength of concrete is its most important characteristic and is also affected by these pores.[25–27)] Research[28)] has shown that total porosity and pore size distribution are the most important factors affecting the compressive strength of samples, and when the proportion of macropores increases, the compressive strength of the sample decreases. Since concrete is porous, the structure is filled with small pores through which water, air, acid and alkali can pass.[29)]

The porosity and pore distribution of geopolymers play an important role in the application of catalyst supports. Previous research[21)] showed that macropores may be formed in the first 4 d. In the present work, potassium and metakaolin-based geopolymer samples were synthesized. The workflow was carried out by evaluating the mechanical strength value and pore size distribution of the geopolymer, which are based on two factors, the varying early-age curing time and air tightness after early-age curing.

2. Experimental

Metakaolin was obtained from Sobue Clay Co. Ltd., Japan, with 1.1 wt% of impurities (mostly TiO_2). Amorphous fumed silicon, SiO_2, called EFACO silica, was purchased from Tomoe Engineering Co., Ltd., Japan.

In order to prepare geopolymer composites, an alkaline solution consisting of KOH powder (UNID.Co.Ltd.), potassium silicate solution, K_2SiO_3 (FUJIFILM Wako Pure Chemical Corporation; concentration 50%) and distilled water was prepared. The composition for making the geopolymer is listed in Table I.

The synthesis process of the geopolymer samples is shown in Fig. 1. EFACO silica powder was added to the solution,

Table I. Curing treatment process.

Group number	Sample number	Curing 1			Curing 2		
		Temperature	Time	Treatment	Temperature	Time	Treatment
1	A	60 °C	1 d	With lid	RT	13 d	With lid
	B						Open lid
2	C		2 d			12 d	With lid
	D						Open lid
3	E		3 d			11 d	With lid
	F						Open lid
4	G		4 d			10 d	With lid
	H						Open lid

which was stirred for 1 min. Then, metakaolin was added to the solution, which was stirred for a further 4 min. Finally, the slurry was stirred for a further 5 min in order to make the mixture homogeneous. After the raw materials were mixed, the slurry was cast in $\varphi 37 \times 60$ mm plastic molds, wrapped with plastic film and sealed with lids to ensure good air tightness. The curing process is shown in Table I. The curing process was divided into two periods. The first one, called Curing 1, was dried at 60 ℃ for various times. The Curing 2 process took place at air temperature, and the time was adjusted so that the total curing time was 14 d. There were eight samples, divided into four groups. Each group comprised two samples, which had the same Curing 1 condition but different treatment in Curing 2. The four groups of samples were removed from the oven and stored at room temperature (20 ℃) and relative humidity 45% ± 5% until tested.

The mass change after 14 d curing was used to calculate the rate of relative weight loss of the sample. A scanning electron microscope (SEM) was used to measure the pores in this study. Cross-section observation specimens were prepared by cutting a sample perpendicular to the longitudinal axis, 7 mm from the bottom and 7 mm from the top. Approximately 300 pores were observed on the cross-sections to analyze the pore size distribution on the bottom and top of the samples.

To analyze phases in the geopolymer, X-ray diffraction (XRD) with Cu-Kα radiation (0.15418 nm) was used with a scanning angle range of 10°–60° (voltage of 40 kV, current of 40 mA, scan speed of 10° min^{-1} and step of 0.02°).

We ground the test surface of each sample for about 5 h to ensure that the surface of the sample could be more accurately measured using a microscope to measure the size of the indentation left on the surface of the sample. A Vickers indenter was loaded at 1 kgf for 15 s with 12 measurements for each sample.

3. Results

The relative weight change of the samples (open lid) in Curing 2 is shown in Fig. 2. After Curing 1 was completed, the weight of all samples decreased faster in 1 or 2 d. However, the relative weight of all samples on the 14th day was about 90% and there was no significant difference. The shrinkage of the samples was obtained by calculating the volume of the 14th day and the initial volume. The results showed that for the samples that were sealed in Curing 2, the shrinkage rate was almost uniform at about 0.5% on the 14th day. For the sample with the lid open in Curing 2, the shrinkage rate of the samples cured at 60 ℃ from 1–4 d in Curing 1 was 2.2%, 2.2%, 2.1% and 2.1%, respectively.

SEM images of geopolymer cured at ℃ with different times in Curing 1 are shown in Fig. 3. When the sample was cured at 60 ℃ for 1 d, the SEM image showed that the porosity is slightly larger than that of the other samples. The pore size distributions are shown in Fig. 4. When the samples were cured at 60 ℃ for the same length of time, the average pore size of the samples with a lid and without a lid was not very different. However, for the samples with the lid open, the average pore size ranged from 1.4×10^2 μm to 2.3×10^2 μm, while for the samples with a lid, the average pore size

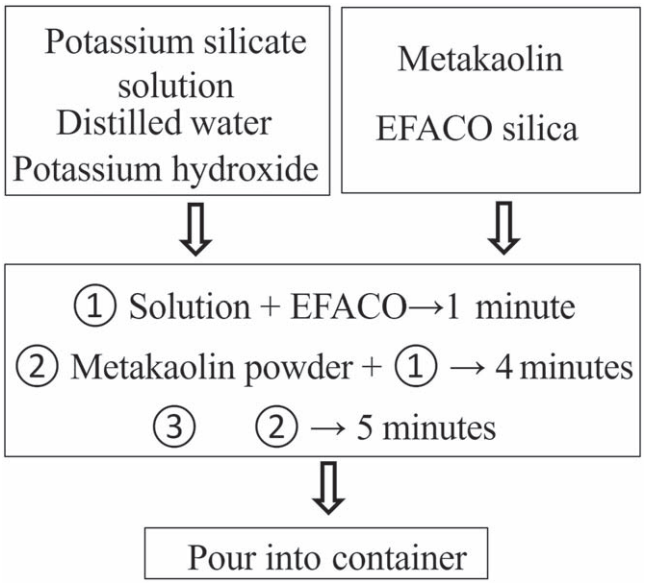

Fig. 1. Synthesis process of the geopolymer samples.

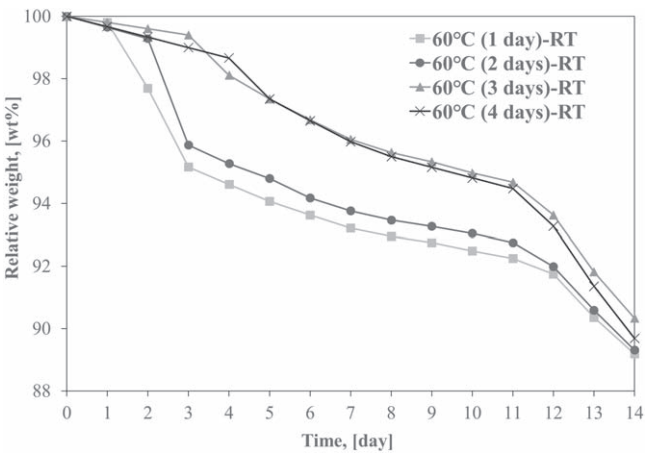

Fig. 2. Relative weight change during post curing.

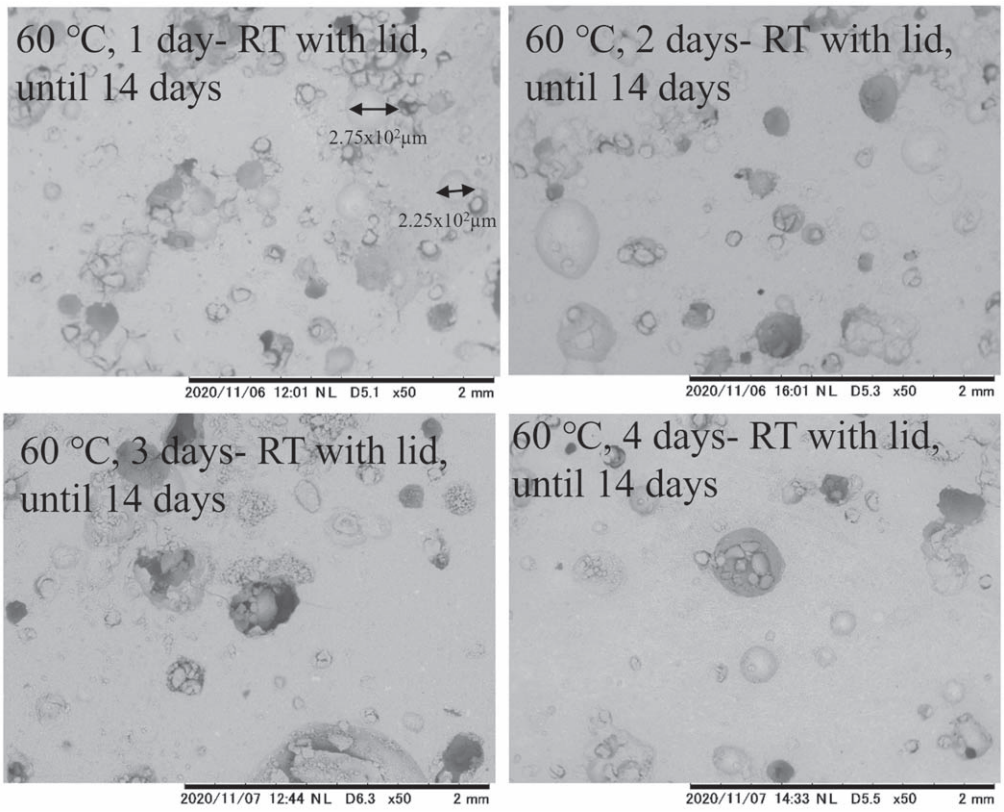

Fig. 3. SEM images of geopolymer cured at ℃ with different time in Curing 1.

was mainly distributed from 0.9×10^2 μm to 2.0×10^2 μm. The average pore size of the samples with a lid tends to be smaller than those without a lid. The pore size of the top and bottom showed that they were mainly distributed from 1.1×10^2 μm to 2.5×10^2 μm. However, in the range from 1.6×10^2 μm to 2.0×10^2 μm, the frequency of the top pore size distribution was 21% significantly higher than that of the bottom.

The XRD patterns, as shown in Fig. 5, indicated that geopolymer was synthesized, and even some illite and $SiO_2 \cdot xH_2O$ crystal peaks appeared in all the samples.

The Vickers hardness is shown in Fig. 6. The error bar of each sample shows that the hardness of the sample is unstable. However, the average Vickers hardness did not change significantly with the increase in the number of days in Curing 1. When the sample was cured for 1 d at 60 ℃, its Vickers hardness on the 14th day had reached a high value.

4. Discussion

As the well-known reaction model assumes,[24] water acts as the medium and participates in several intermediate reactions during geopolymer formation, such as dissolution, polycondensation, etc. A previous report showed that water could exist inside the final products as free or bound water, and thus had an influence on the microstructure.[30] In this study, the relative weight change on the 14th day of metakaolin and potassium-based geopolymer was within 10% difference and was not affected by the length of curing time at 60 ℃ in Curing 1. We infer that the samples may have formed similar microstructures under different curing times in Curing 1. XRD results showed that illite and $SiO_2 \cdot xH_2O$ were detected in all samples, confirming the similar microstructure mentioned earlier. The shift of the amorphous halo from $2\Theta_{max} = 22°$ in the metakaolin processor to $2\Theta_{max} = 27–30°$ in the cured geopolymer samples has been commonly explained by structural changes caused in aluminosilicates during geopolymerization.[5,24]

The SEM image showed a slight increase in porosity in the sample cured for a shorter time in Curing 1. Figures 4(a) and 4(b) showed that regardless of whether the samples had a lid or not, a higher frequency of small pores appeared in the sample with a short curing time in Curing 1. However, the average pore sizes were not very different. Figures 4(c) and 4(d) showed that the distribution of pores at the top tends to be larger. The top pore distribution of all samples showed greater consistency. Figure 4(a) showed that the pores at the bottom tend to be larger as the curing time increases in Curing 1. However, the performance of the average pore size is almost the same, and the Vickers hardness of the geopolymer samples did not change. A report[23] showed that the produced geopolymer samples can reach high compressive strength after heating at 60 °C for 12 h. This experiment showed that the Vickers hardness of geopolymers can reach a high value of about 90 MPa in 1 d.

5. Conclusion

Synthesis and dehydration of potassium and metakaolin-based geopolymer were carried out. The pore size distribution and Vickers hardness of geopolymers under different early curing time and air tightness have been studied.

This study shows that when the sample is cured at 60 °C for 1–4 d and the air tightness is subsequently changed, the shrinkage rate remains relatively consistent, at about only 2.1%. We infer that potassium and metakaolin-based

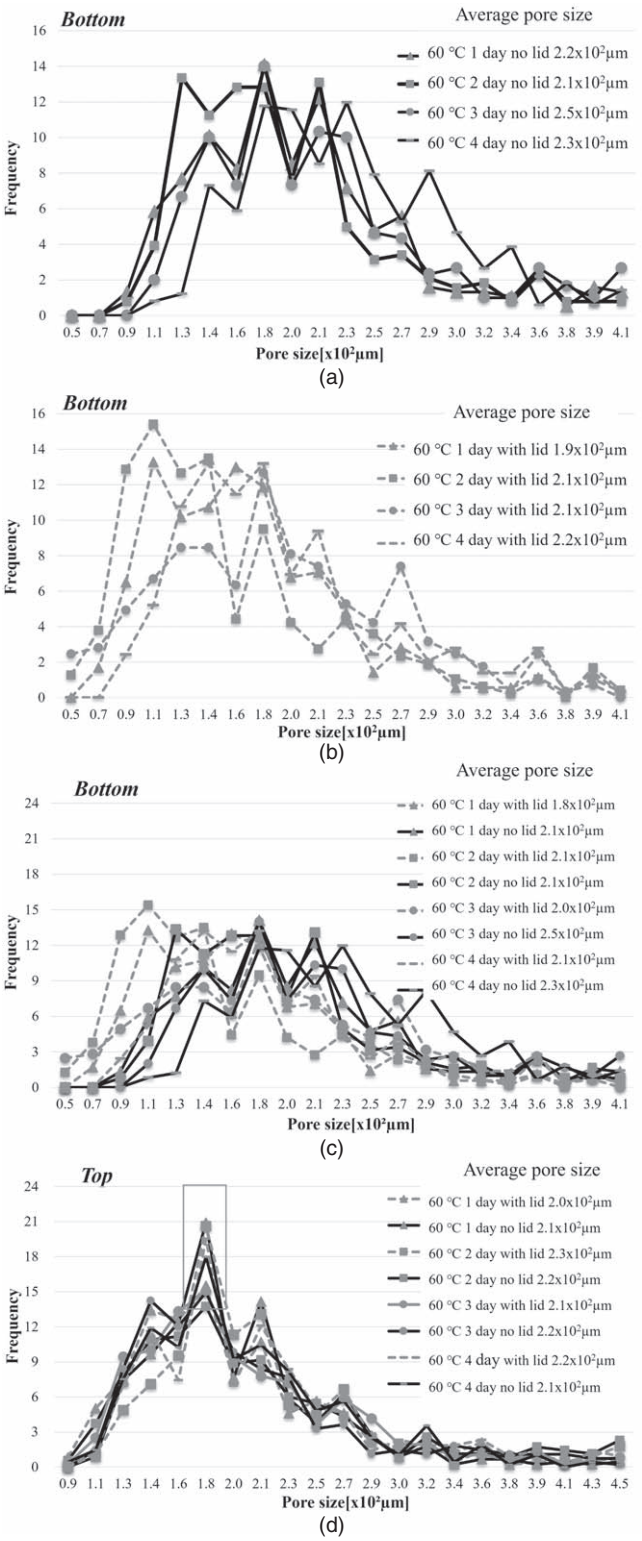

Fig. 4. Pore size distributions. "(a)" and "(b)" are the pore size distribution on the bottom part of the samples cured with no lid and with a lid. "(b)" and "(d)" are the pore size distribution on the bottom and top part for all the samples.

geopolymer has low shrinkage performance and is not affected by the length of early curing time.

The results of the Vickers hardness test showed that the sample was cured at 60 °C for 1 d, and the Vickers hardness on the 14th day had reached 90 MPa. Longer early curing did not significantly change the Vickers hardness on the 14th day.

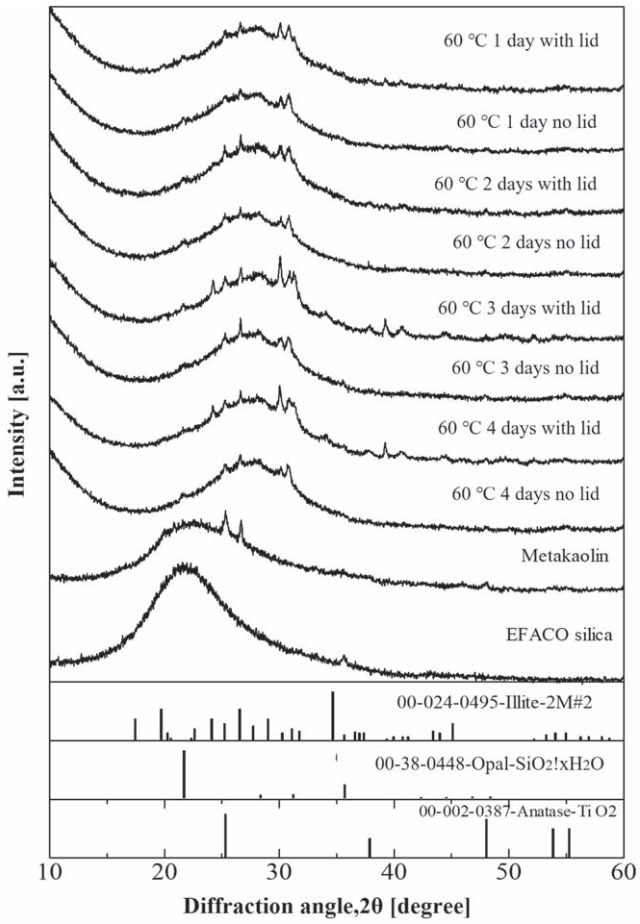

Fig. 5. XRD pattern of geopolymer under different conditions.

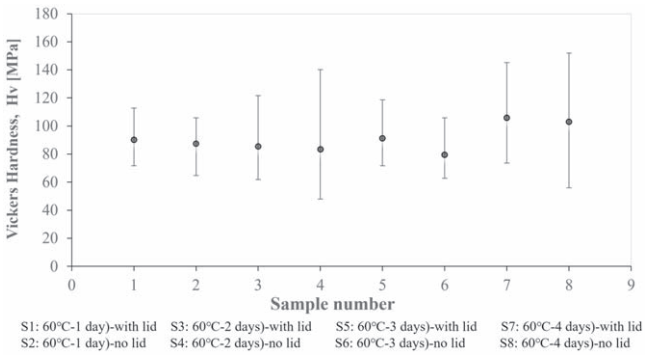

Fig. 6. Vickers hardness of geopolymer synthesized under different conditions.

The results of pore distribution and average pores size show that the pore size distribution at the top tends to be larger compared to that at the bottom. As the early-age curing time at 60 °C increases, the pore distribution at the bottom tends to be large pores, while the pore distribution at the top shows greater consistency. However, for all samples, the average pore size is almost the same at about 2.1×10^2 μm.

Acknowledgments

This work was supported by ADVAN ENG. Co., Ltd.

ORCID iDs

Yaru Yang https://orcid.org/0000-0002-3170-3572

Hisayuki Suematsu https://orcid.org/0000-0003-4680-3266

1) Technical Strategic Plan 2017 for Decommissioning of the Fukushima Daiichi Nuclear Power Station of Tokyo Electric Power Company Holdings, Inc Nuclear Damage Compensation and Decommissioning Facilitation Corporation, 2017, Fukushima Nuclear Accident Archive[https://f-archive.jaea.go.jp/dspace/handle/faa/172450].
2) T. Utsumi et al., "Preparation of potassium and metakaolin based geopolymer foam with millimeter sized open pores for hydrogen recombining catalyst supports," J. Ceram. Soc. Jpn. **128**, 96 (2020).
3) J. O. Henrie and J. N. Appel, Evaluation of special safety issues associated with handling the Three Mile Island Unit 2 core debris, University of North Texas Libraries, 1985, Richland, Washington, UNT Digital Library [https://digital.library.unt.edu/ark:/67531/metadc1096962/].
4) J. Davidovits, "Global Warming Impact on the Cement and Aggregates Industries," World Resource Rev. **6**, 263–278, [https://www.researchgate.net/publication/236503901_Global_Warming_Impact_on_the_Cement_and_Aggregates_Industries] (1994), Geopolymer Institute, France.
5) P. Duxson et al., "Geopolymer technology: the current state of the art," J. Mater. Sci. **42**, 2917 (2007).
6) E. J. Guades et al., "Compressive strength of geopolymer concrete: influence of size of gravel," 6th Int. J. Adv. Eng. Sci. Conf. on Appl. Math 2016, 10.15242/IIE.E1216009.
7) D. Hardjito and B. V. Rangan, "Development and properties of low-calcium fly ash-based geopolymer concrete," Curtin Research Publications **94**, 19327 (2005), [http://hdl.handle.net/20.500.11937/5594].
8) T. F. Pacheco et al., "Alkali-activated binders: a review: I. Historical background, terminology, reaction mechanisms and hydration products," Constr. Build. Mater. **22**, 1305 (2008).
9) T. García-Mejía et al., "Compressive strength of metakaolin-based geopolymers: influence of KOH concentration, temperature, time and relative humidity," Mater. Sci. Appl. **7**, 772 (2016).
10) Z. Zhang and H. Wang, "The pore characteristics of geopolymer foam concrete and their impact on the compressive strength and modulus," Frontiers in Materials Build. Mater **24**, 1176 (2016).
11) D. Partha, N. Pradip, and S. Prabir, "Drying shrinkage of slag blended fly ash geopolymer concrete cured at room temperature," Procedia Eng. **125**, 594 (2015).
12) V. F. F. Barbosa and K. J. D. Mackenzie, "Thermal behaviour of inorganic geopolymers and composites derived from sodium polysialate," Mater. Res. Bull. **38**, 319 (2003).
13) J. Feng, R. Zhang, L. Gong, Y. Li, W. Cao, and X. Cheng, "Development of porous fly ash-based geopolymer with low thermal conductivity," Materials & Design (1980-2015) **65**, 529 (2015).
14) Y. H. Jia et al., "Study on Setting Time of Fly Ash-based Geopolymer," Bull. Chin. Ceram. Soc. **28** [5] , 893–899 (2009), [http://gsytb.jtxb.cn/EN/Y2009/V28/I5/893].
15) W. H. Tao et al., "Studies on Properties and Mechanisms of Geopolymer Cementitious Material," Bull. Chin. Ceram. Soc. **4**, 730 (2008), [http://gsytb.jtxb.cn/EN/Y2008/V27/I4/730].
16) T. Bakharev, "Resistance of geopolymer materials to acid attack," Cem. Concr. Res. **35**, 658 (2005).
17) J. Davidovits, "Geopolymers: inorganic polymeric new material," J. Therm. Anal. **37**, 1633 (1991).
18) E. Lyon, P. N. Balaguru, A. Foden, U. Sorathia, J. Davidovits, and M. Davidovits, "Fire resistant aluminosilicate composites," Fire Mater. **21**, 67 (1997).
19) H. Xu and J. S. J. Van Deventer, "The geopolymerisation of alumino-silicate minerals," Int. J. Miner. Process. **59**, 247 (2000).
20) D. Sumajouw, D. Hardjito, S. Wallah, and B. Rangan, "Fly ash-based geopolymer concrete: study of slender reinforced columns," J. Mater. Sci. **42**, 3124 (2007).
21) Y. Yang, T.-C. Le, I. Kudo, T.-M. Do, K. Niihara, H. Suematsu, and G. Thorogood, "Pore forming process in dehydration of metakaolin-based geopolymer," Int. J. Ceram. Eng. Sci. **3** [5] , 211–216 (2021).
22) P. Rovnaník, "Effect of curing temperature on the development of hard structure of metakaolin-based geopolymer," Constr. Build. Mater. **24**, 1176 (2010).
23) H. L. Chi et al., "Preparation and mechanical properties of potassium metakaolin based geopolymer paste," Adv. Eng. Forum **31**, 38 (2019).
24) J. Davidovits, *Geopolymer Chemistry and Applications* (Geopolymer Institute, Saint-Quentin, France, 2011) 3rd. ed., [https://books.google.co.in/books?id=mJBotwAACAAJ].
25) C. Lian, Y. Zhuge, and S. Beecham, "The relationship between porosity and strength for porous concrete," Constr. Build. Mater. **25**, 4294 (2011).
26) S. Zhang, K. Cao, C. Wang, X. Wang, G. Deng, and P. Wei, "Influence of the porosity and pore size on the compressive and splitting strengths of cellular concrete with millimeter-size pores," Constr. Build. Mater. **235**, 117508 (2020).
27) S. Mindess, "Relation between the compressive strength and porosity of autoclaved calcium silicate hydrates," J. Am. Ceram. Soc. **53**, 621 (1970).
28) Z. F. Farhana, H. Kamarudin, A. Rahmat, and A. M. M. Al Bakri, "A study on relationship between porosity and compressive strength for geopolymer paste," Key Eng. Mater. **594–595**, 1112 (2013).
29) K. Rakesh and B. Bishwajit, "Porosity, pore size distribution and in situ strength of concrete," Cem. Concr. Res. **33**, 155 (2003).
30) M. Lizcano, A. Gonzalez, S. Basu, K. Lozano, and M. Radovic, "Effects of water content and chemical composition on structural properties of alkaline activated metakaolin-based geopolymers," J. Am. Ceram. Soc. **95**, 2169 (2012).